Ecography

ECOG-05191
Hoeks, S., Huijbregts, M. A. J., Busana, M.,Harfoot, M. B. J., Svenning, J.-C. and Santini, L. 2020. Mechanistic insights into the role of large carnivores for ecosystem structure and functioning. – Ecography doi: 10.1111/ecog.05191

Supplementary material

Supplementary material Appendix 1

In order to utilize the Madingley model for studying the effect of removing large carnivores from ecosystems (i.e. removing the top-down control), a few minor updates were applied to the original model first presented by Harfoot et al. (2014). We choose to use the C++ version of the source code in order to run our analysis on a Linux cluster (Cartesius HPC at Surfsara). The alterations made to the C++ source code are explained in the sections below and the updated source code can be retrieved from: https://github.com/Shoeks/MadindingCPP. Supplementary material Appendix Table A1 provides a summarized overview of alterations.

Optimum predator-prey ratio

In the Madingley model the attack rates of predators (for both omnivores and carnivores) on other heterotrophs are determined from the size-structured model of Williams et al. (2010), where the probability of predation is a function of the optimal prey body size (which is defined as a proportion of predator size). The effective rate at which an individual predator searches its environment and successfully kills prey (denoted as $a_{i,j}$) can be computed using the following equation:

$$\alpha_{i,j} = \alpha_0^{pred} . M_{i,(t)} . \varpi_{i,j} \qquad \text{Equation 1}$$

Where $\varpi_{i,j}$ is the probability of successfully capturing a prey item, which was modelled following assuming that the probability of a predator capturing prey of some proportion of its own body mass follows the following distribution:

$$\varpi_{i,j} = \exp\left[-\left(\frac{\ln\left(\frac{M_{j,(t*)}}{M_{i,(t)}}\right) - \ln\left(\theta_i^{opt}\right)}{\sigma_{pred-prey}^{opt}}\right)^2\right]. \qquad \text{Equation 2}$$

Where $M_{j,(t*)}$ and $M_{i,(t)}$ are the body masses of the prey and predator, respectively. θ_i^{opt} reflects the optimal predator-prey body mass ratio and $\sigma_{pred-prey}^{opt}$ sets the standard deviation. In the original version of the Madingley model the average $\theta_i^{opt}$was set to 0.1 (e.g. Harfoot et al., 2014; Newbold et al., 2018) which caused all predators to have a prey preference of 10% of their own body mass. Although an average optimal predator-prey ratio of 0.1 might be a meaningful value for most of the carnivorous fauna, Carbone et al. (1999), Carbone et al. (2007) and Tucker et al. (2016) have shown that this relationship shifts after carnivore body mass exceeds a certain threshold. For these larger carnivores (>21 kg) an average $\theta_i^{opt}$of 1 is more appropriate according Carbone et al. (1999). Carnivores in the category of large carnivores are, generally speaking, more likely to feed on prey close to their own body mass.

Under the default predation parameters in the Madingley (θ_i^{opt} = 0.1, $\sigma_{pred-prey}^{opt}$= 0.7) (Harfoot et al., 2014) carnivorous cohort with an average body mass of 100 kg can effectively predate on prey cohorts ranging from roughly 2.5 to 25 kg. With the updated parameters (θ_i^{opt} = 1.0, $\sigma_{pred-prey}^{opt}$= 0.7), which only apply to endothermic carnivorous cohorts, the same carnivorous cohort with an average body mass of 100 kg is able to effectively predate on prey cohorts ranging from 25 to 250 kg. Predation outside this range is possible ($\varpi_{i,j}$is a continuous distribution), the likeliness to successfully capture a prey cohort is very small. However, $M_{j,(t*)}$ (body mass prey) and $M_{i,(t)}$ (body mass predator) both consider the average cohort body mass at the current time step, thus a given predator might be able to feed on very large preys when the prey cohort has not yet reached its potential adult body mass (i.e. juvenile cohorts). In our simulations, this resulted in megaherbivores (≥1000 kg) being

exclusively predated when the representative cohort is in the juvenile stage (when its average body mass was <1000 kg). This is therefore in line with to studies stating that megaherbivores are often either too difficult or too risky to catch, even by the largest predators (Fritz et al. 2011, Malhi et al. 2016, le Roux et al. 2019).

Omnivore diet restriction

In the original version of the Madingley, omnivores do better than carnivores where productivity is lower as the advantage of dietary flexibility when meat is scarce, i.e. the ability to survive on plant matter, outweighs their disadvantage of lower assimilation efficiency of animal matter when it is available. Carnivores do better than omnivores where productivity is higher for the opposite reason, their advantage in assimilation efficiency outweighs their disadvantage in flexibility. Despite the fact that this might be realistic in some cases, the method by which the flexibility of omnivores is currently implemented causes oddities when studying extinctions of megacarnivores, as large omnivores can effectively take the role of large carnivores once these go extinct. Therefore, we applied a simple rule to the feeding behaviour of omnivores: omnivore diet restricted to heterotrophs with a maximum size of 25% compared to their own body weight, which results in confining omnivores to feed mostly on small endotherms and ectotherms

Spatial cohort body mass initialization

In the default model each cohort is initialized by selecting its functional group (see main text Table 1) and sampling an adult body mass from a log-normal distribution confined between a maximum and minimum body mass. These body mass boundaries are set using one of the input files and are not spatially explicit. In order

to refine the initialized body mass ranges, we updated the model by including a function that sets the maximum possible body mass per functional group in a spatially explicit manner using maximum body mass masks stored as netCDF files. For our simulations the body mass masks for endotherms (Supplementary material Appendix Fig. A1) were constructed by combining body mass information extracted from the EltonTraits 1.0 database (Wilman et al., 2014) and the species ranges from the IUCN Red List (2018). For ectotherms (Supplementary material Appendix Fig. A1), we used data for reptiles and combined body mass data from the amniote life-history database (Myhrvold et al., 2015) with the species ranges from the GARD initiative (Roll et al., 2017).

Table A1 Summary of changes applied to the Madingley Model

Updates	Short summary
1. Optimum predator-prey ratio (see section 1.1)	• Large endothermic predators (>21 kg) have an average optimal prey-predator body mass ratio of θ_i^{opt} = 1 • Smaller predators and all ectotherms retain the default ratio of θ_i^{opt} = 0.1
2. Omnivore diet restrictions (see section 1.2)	• Omnivore diet restricted to feed on small prey
3. Madingley output writing	• Writing and summarizing data for food-web plots • Writing summarized biomass and abundance timelines • Exporting model state for re-initialization
4. (Re)-initialization	• Function that allows re-initialization using a previously created model state • Functional group maximum body masses are initialized spatially (netCDF inputs) (see section 1.3) • Added C++ flags allow for easy batch simulations
5. Increase computational efficiency	• Improved cohort searching algorithm (faster predation) • Restructured parts of the ported C++ code

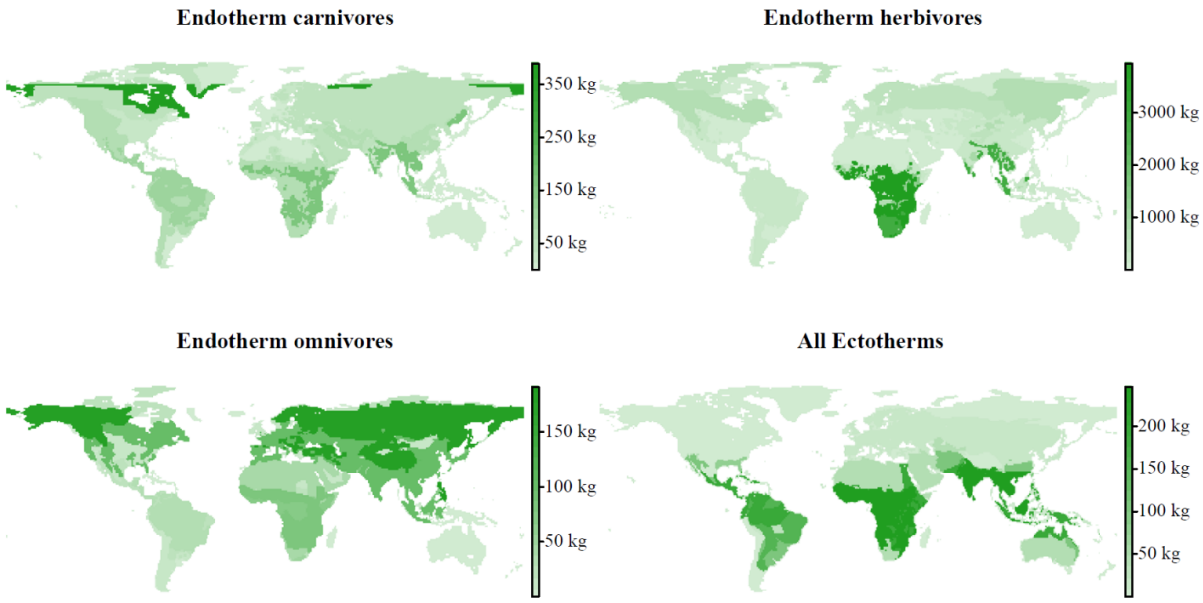

Figure A1. Maximum body masses (in kg) used for initializing cohorts in each grid cell.

Supplementary material Appendix 2

Random forest approach

We ran six random forest models to assess the global influence of net primary productivity (NPP) and seasonality (NPPsd; quantified by the yearly standard deviation of NPP) on the relative response of autotrophs, herbivores, omnivores and carnivores after removing the large (>21 kg) carnivores. The models were fitted using the randomForest package in R (Liaw and Wiener 2002). All six random forest models were run independently using the grid cell specific yearly every sum of biomass of: 1) all herbivores, 2) large (>100 kg) endothermic herbivores, 3) small endothermic herbivores, 4) all omnivores, 5) autotrophs and 6) medium-sized (10-21 kg) endothermic carnivores as response variables. For all six models NPP and the yearly NPPsd were used as explanatory variables. All random forest models were run with 1000 trees. The optimal value of the mtry input parameter (mtry = 1) was found using the tuneRF function in the randomForest package. The variable importance of NPP and NPPsd was quantified using the increase in the mean squared error (MSE) of the predictions. Partial responses were smoothened with Loess fits to increase the readability of the plots. The smoothing parameter (α) was set to 0.5. Fig. A2 and Fig. A3 show the partial response plots of NPP and NPPsd for all six random forest models.

Random forest results

The relative change in biomass of all herbivores after the removal of large carnivores was positively related to NPP (Fig A2a) and negatively related with NPPsd (Fig A2d). This indicates that the response of herbivore biomass, following the removal of large carnivores, is stronger in environments characterized by high NPP and low seasonality. A similar observation holds when only considering the large (>100 kg) endothermic herbivores (Fig. A2b,e). Finally, smaller endothermic herbivore also shows a similar, but weaker, response (Fig. A2c and Fig. A2f).

The response of omnivores (Fig. A3a,d) was similar to that of herbivores. However, at higher levels of NPP (> 2.5 gC/m2/day) the relationship turns to negative, possibly because of the increased competition with more efficient herbivores and carnivores.

The increase in mesopredators (medium-sized (10-21 kg) endothermic carnivores) was more pronounced at higher levels of NPP (Fig. A3c) and decreased with increased NPPsd (Fig. A3f), suggesting that the response of mesopredators may be stronger in environments characterized by high NPP and low seasonality.

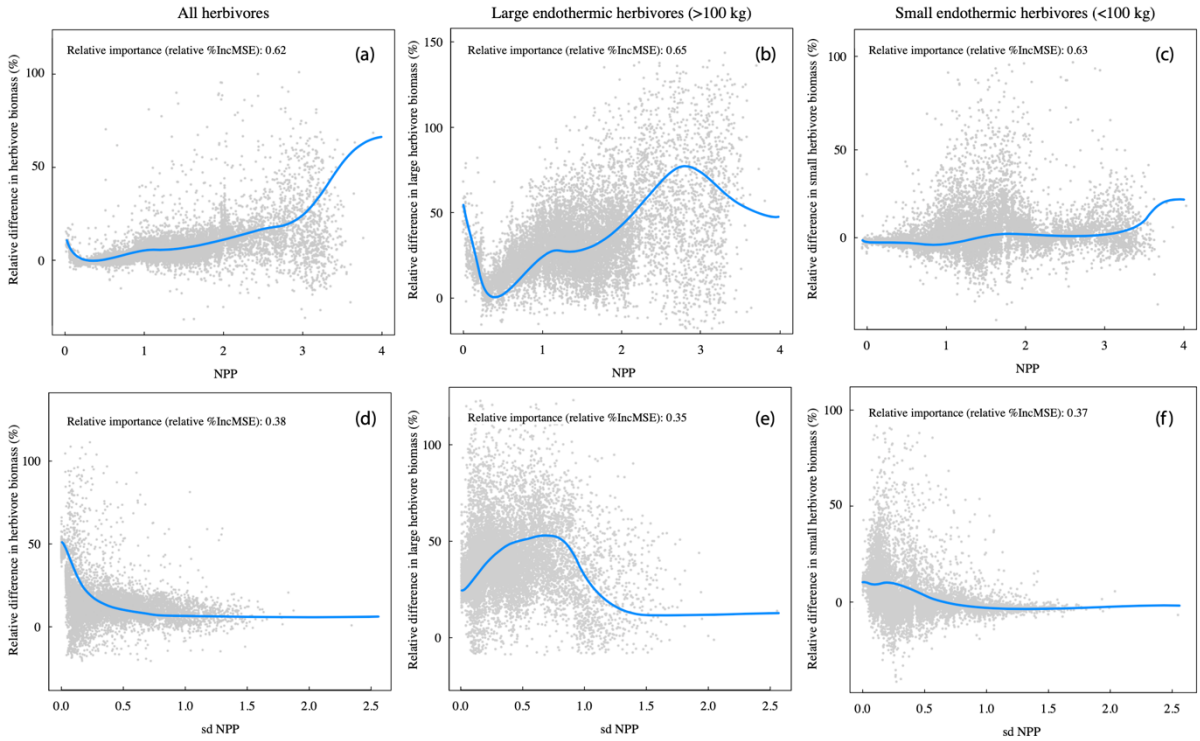

Figure A2. Partial response plots for three random forest models fitted on the global simulation results. All models were trained using two explanatory variables: 1) NPP quantified in gC/m2/day (a, b, and c) and 2) the yearly standard deviation in NPP (d, e, f). Each model was trained with a single response variable, the following three response variables were used for each of the three random forest models independently: 1) the relative change in biomass of all herbivores (a and d), 2) the relative change in biomass of all large (>100 kg) endothermic herbivores (b and e) and 3) the relative change in biomass of all smaller (<100 kg) endothermic herbivores (c and f) following the removal of large carnivores. Fits were smoothened by fitting a Loess function through the partial response results.

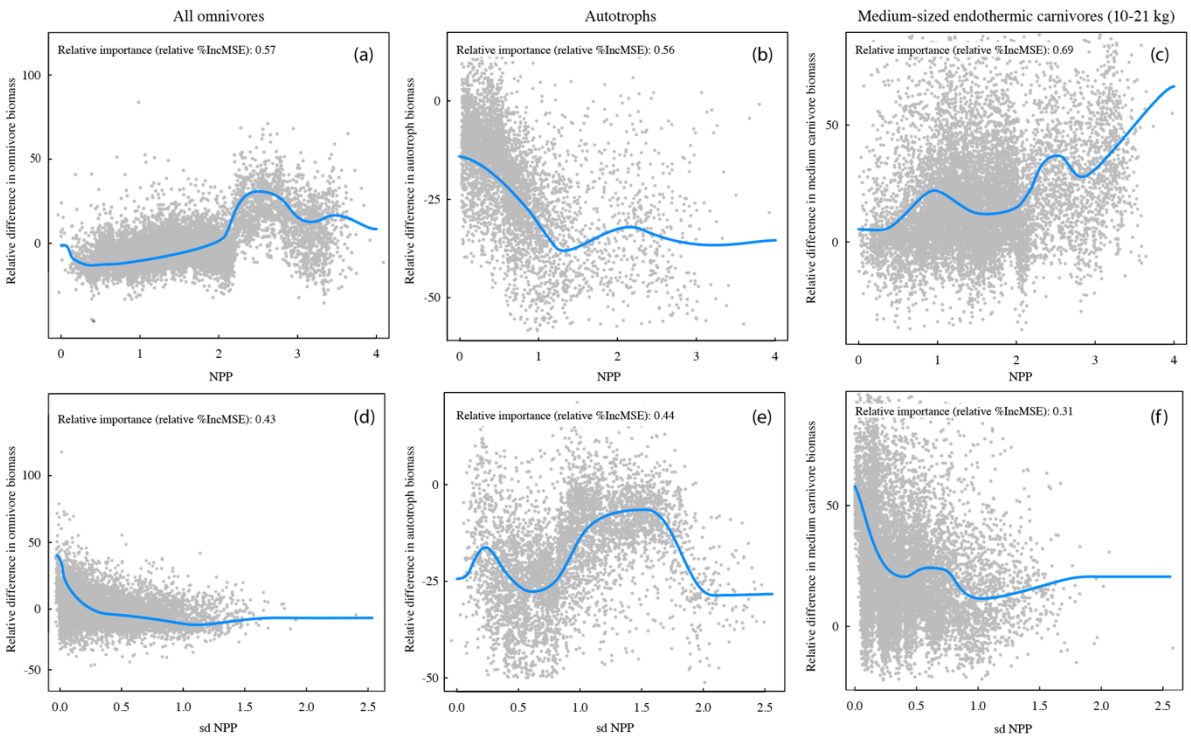

Figure A3. Partial response plots for three random forest models fitted on the global simulation results. All models were trained using two explanatory variables: 1) NPP quantified in gC/m2/day (a, b, and c) and 2) the yearly standard deviation in NPP (d, e, f). Each model was trained with a single response variable, the following three response variables were used for each of the three random forest models independently: 1) the relative change in biomass of all omnivores (a and d), 2) the relative change autotroph biomass (b and e) and 3) the relative change in biomass of medium-sized (10-21 kg) endothermic carnivores (c and f) following the removal of large carnivores. Fits were smoothened by fitting a Loess function through the partial response results.

Supplementary material Appendix 3

We selected four locations by dividing the Madingley climate inputs (Harfoot et al., 2014; Newbold et al., 2018) into four categories. First, we used the rounded global average of the terrestrial net primary productivity layer (1 gC/m2/day) as a threshold value for dividing the areas into low and high net primary productivity (NPP). The two resulting categories were then further divided into the final set of four climate categories by considering seasonality. From each of the four climate subsets we selected a single location (see Table 2 and Supplementary material Appendix Fig. A4). The closest national park as well as country name is presented as a point of reference. Each of the four selected areas consists of an isolated area of 5 grid cells by 5 grid cells, at a 1-degree resolution. Movement in or out the designated area is not considered. As with the global simulations, no land use changes were imposed in the model.

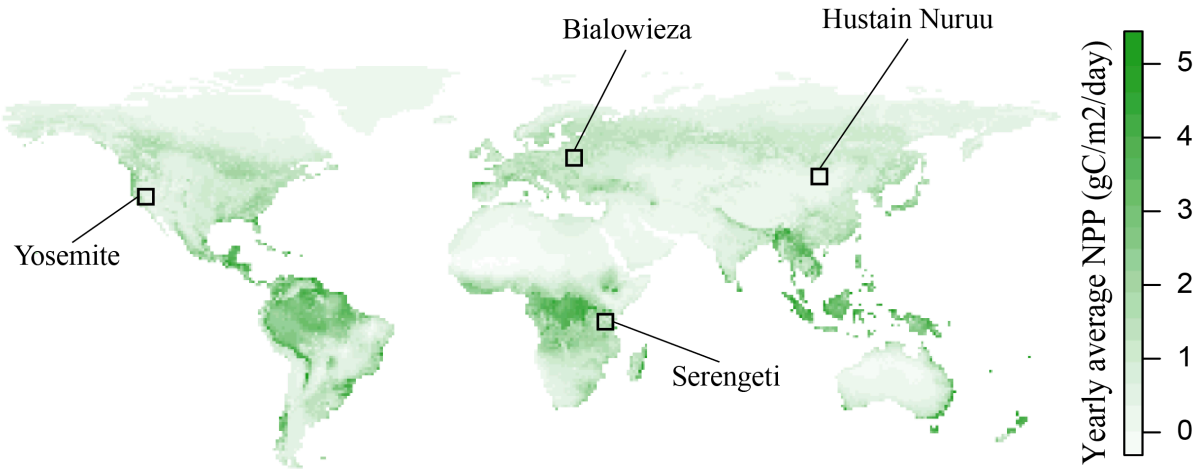

Figure A4. Small-scale simulation locations plotted on top of the yearly average NPP (gC/m^2/day).

Supplementary material Appendix 4

We ran spin-ups for a period of 500 years without any interferences to let the model stabilize. The 500-year simulation spin-up period was sufficient to allow the model to converge to a stable state (Fig. A5).

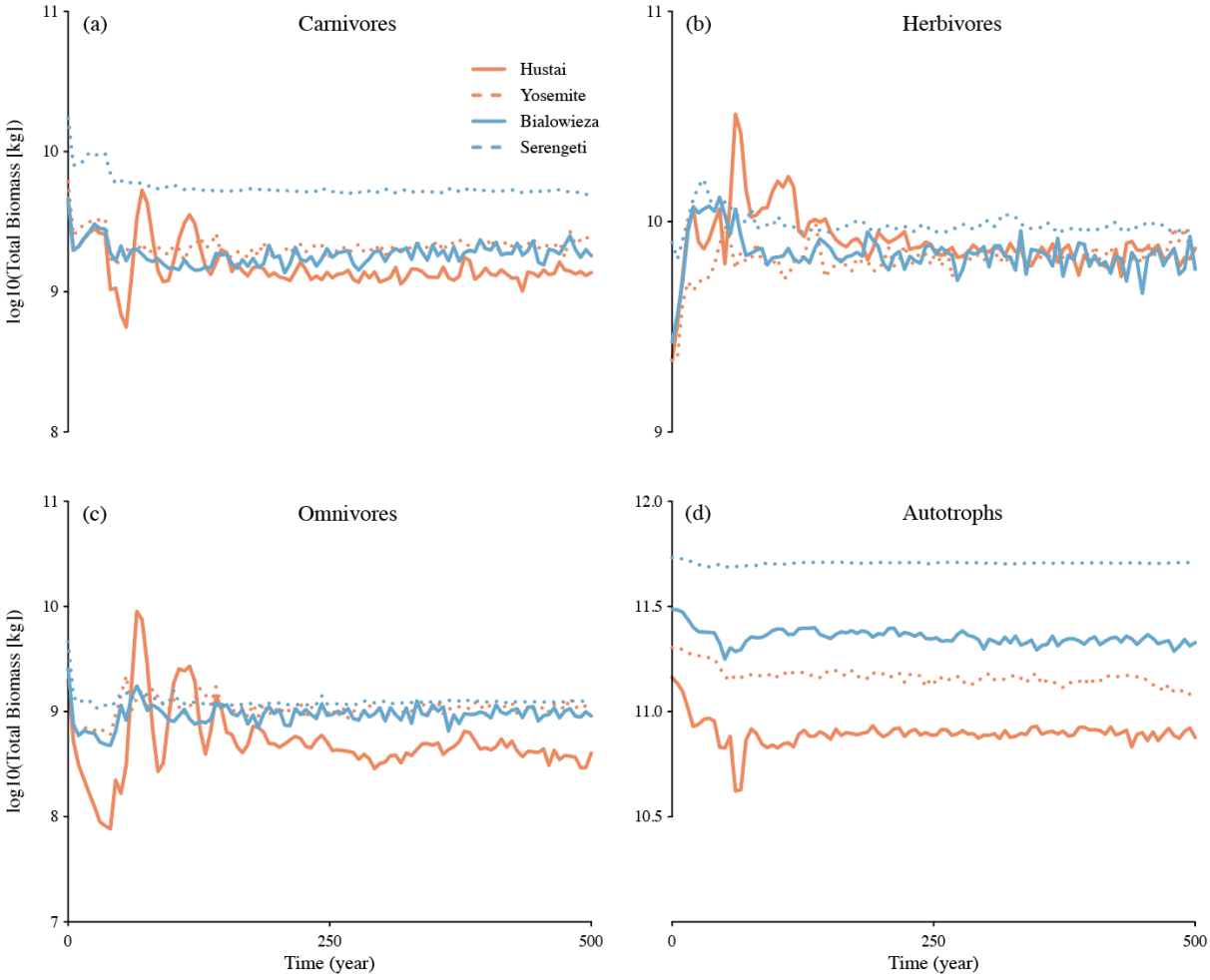

Figure A5. The total $\log_{10}$ biomass (kg) over time of (a) carnivores, (b) herbivores, (c) omnivores and (d) autotrophs before the removal of large (>21 kg) carnivores for four small-scale simulations. The time series are averaged across 5 simulation replicas. The four small-scale simulations were modelled under four climate conditions found in: 1) the Hustai Nuruu (solid orange lines), 2) Yosemite (dashed orange lines), 3) Białowieża (solid blue lines) and 4) the Serengeti (solid blue lines) (see Table 2 in main text).

References supporting information

Harfoot MB, Newbold T, Tittensor DP, Emmott S, Hutton J, Lyutsarev V, Smith MJ, Scharlemann JP, Purves DW. Emergent global patterns of ecosystem structure and function from a mechanistic general ecosystem model. PLoS biology. 2014; 12(4):e1001841.

Williams RJ, Anandanadesan A, Purves D. The probabilistic niche model reveals the niche structure and role of body size in a complex food web. PloS one. 2010 Aug 9;5(8):e12092.

Newbold T, Tittensor DP, Harfoot MB, Scharlemann JP, Purves DW. Non-linear changes in modelled terrestrial ecosystems subjected to perturbations. bioRxiv. 2018 Jan 1:439059.

Carbone C, Mace GM, Roberts SC, Macdonald DW. Energetic constraints on the diet of terrestrial carnivores. Nature. 1999; 402(6759):286.

Carbone C, Rowcliffe JM, Cowlishaw G, Isaac NJ. The scaling of abundance in consumers and their resources: implications for the energy equivalence rule. The American Naturalist. 2007 Jul 19;170(3):479-84.

Tucker MA, Ord TJ, Rogers TL. Revisiting the cost of carnivory in mammals. Journal of evolutionary biology. 2016 Nov;29(11):2181-90.

Wilman H, Belmaker J, Simpson J, de la Rosa C, Rivadeneira MM, Jetz W. EltonTraits 1.0: Species-level foraging attributes of the world's birds and mammals: Ecological Archives E095-178. Ecology. 2014; 95:2027-2027

IUCN. The IUCN red list of threatened species. Version 2018-1; 2018 [cited 2019 May 14]. Available from http://www.iucnredlist.org.

Myhrvold NP, Baldridge E, Chan B, Sivam D, Freeman DL, Ernest SM. An amniote life-history database to perform comparative analyses with birds, mammals, and reptiles: Ecological Archives E096-269. Ecology. 2015 Nov;96(11):3109-.

Roll U, Feldman A, Novosolov M, Allison A, Bauer AM, Bernard R, Böhm M, Castro-Herrera F, Chirio L, Collen B, Colli GR. The global distribution of tetrapods reveals a need for targeted reptile conservation. Nature Ecology & Evolution. 2017 Nov;1(11):1677.

Liaw A, Wiener M. Classification and regression by randomForest. R news. 2002 Dec 3;2(3):18-22.